ACS APPLIED MATERIALS & INTERFACES

Research Article

www.acsami.org

Direct Writing on Paper of Foldable Capacitive Touch Pads with Silver Nanowire Inks

Ruo-Zhou Li,[†,‡,§] Anming Hu,[*,†] Tong Zhang,[‡,§] and Ken D. Oakes[∥]

[†]Department of Mechanical, Aerospace and Biomedical Engineering, University of Tennessee, Knoxville 37996, United States

[‡]Key Laboratory of Micro-Inertial Instrument and Advanced Navigation Technology, Ministry of Education, School of Electronic Science and Engineering, Southeast University, Nanjing 210096, China

[§]Suzhou Key Laboratory of Metal Nano-Optoelectronic Technology, Suzhou Research Institute of Southeast University, Suzhou 215123, China

[∥]Verschuren Centre, Department of Biology, Cape Breton University, 1250 Grand Lake Road, Sydney, B1P 6L2 Canada

Supporting Information

ABSTRACT: Paper-based capacitive touch pads can be fabricated utilizing high-concentration silver nanowire inks needle-printed directly onto paper substrates through a 2D programmable platform. Post deposition, silver nanowire tracks can be photonically sintered using a camera flash to reduce sheet resistance similar to thermal sintering approaches. Touch pad sensors on a variety of paper substrates can be achieved with optimized silver nanowire tracks. Rolling and folding trials, which yielded only modest changes in capacitance and no loss of function, coupled with touch pad functionality on curved surfaces, suggest sufficient flexibility and durability for paper substrate touch pads to be used in diverse applications. A simplified model to predict touch pad capacitance variation ranges with differing touch conditions was developed, with good agreement against experimental results. Such paper-based touch pads have the advantage of simple structure, easy fabrication, and fast sintering, which holds promise for numerous commercial applications including low-cost portable devices where ultrathin and lightweight features, coupled with reliable bending stability are desirable.

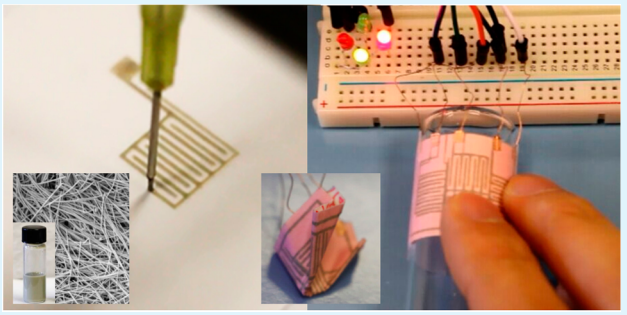

KEYWORDS: *direct writing, silver nanowire inks, paper, touch sensors, flexible electronics*

1. INTRODUCTION

Cellulose-based paper, inexpensive and commonly available worldwide for information storage and packaging, also holds great promise as a biodegradable substrate for flexible electronics. Although paper is easily modified chemically, it can also be physically formed to complex and compact 3D structures by folding,[1−4] but more importantly, functionalized by a variety of printing techniques.[1] Recently, extensive research has been conducted to evaluate the potential of "paper electronics" including the development of proof-of-concept electronic components such as transistors,[5,6] displays,[7] solar cells,[8,9] batteries,[10] supercapacitors,[11] and electronic memory devices.[12] Nevertheless, few studies to date have investigated the possibility of paper-based touch pads as input devices or for use in interface control applications.[13]

Notably, paper-based actuators and sensors, recognized as "smart paper" or "lab on paper" (LOP) devices, currently play an important role in disposable health industry point-of-care (POC) bedside applications.[14−16] A recent POC analytical platform integrated an internal chemiluminescent light source, fluidic delay-switch, supercapacitor amplifier and metallic electrodes to enable automatic and portable DNA detection.[17] This and similar devices reveal a trend toward incorporating differing sensors and electronic components onto a single paper substrate to produce high-density integrated systems.[14] To fabricate such devices, complicated lithography techniques have been developed to construct paper substrate touch pads. Although the paper substrate costs are negligible, these lithography techniques currently do not result in low-cost devices, as associated manufacturing costs are still quite high.

As a matrix, silver nanowire ink shows much higher conductivity than organic conducting materials such as PEDOTs and CNTs, and silver nanowires demonstrate better chemical stability than Cu or Al nanoinks.[18,19] Notably, silver nanowires can form reticular structures tolerating significant strains because of their superior mechanical properties,[20,21] facilitating development of foldable sensors with electrodes capable of withstanding extremely small bending radii without compromising electrical properties.[21,22]

Received: October 10, 2014
Accepted: November 3, 2014
Published: November 3, 2014

Although paper substrates offer many advantages, they cannot tolerate temperatures above 150 °C, temperatures at which silver nanowire inks are sintered to reduce sheet resistance and enhance conductivity.[22,23] There are various low-temperature sintering processes, such as pressure-assisted sintering[21] or chemical sintering,[24] which will create "hot points" only at the joints between silver nanowires.[22] Such localized heating,[22] conducted at room temperatures, can sinter overlapping nanowires and reduce electrical resistance without damaging the paper substrate by utilizing several millisecond duration photonic pulses at an appropriate intensity.

Herein, we present a facile, rapid approach (requiring only a few minutes) to fabricate a foldable capacitive touch pad. To the best of our knowledge, there are no previous reports describing direct writing using silver nanowire inks on paper through a programmed 2D platform. The influences of paper substrate on directly deposited silver nanowire thickness and electrical properties, prior to and following in situ sintering, was investigated with touch pads of various geometries and compared with detailed theoretical designs and experimental analyses. A simplified model was developed to predict the capacitance variation range of the fabricated touch pads and a rolling test was implemented to evaluate the stability of the silver nanowire tracks on paper-based substrates as a surrogate for anticipated use in mobile device applications.

2. OPERATING PRINCIPLE

Currently, touchpad or tactile sensors are based on various techniques, with resistive,[25] capacitive,[13,26] infrared-sensitive,[27] or triboelectric[28] protocols. Resistive tactile sensors are devised to detect the resistance change with the deformations of membranes or cantilevers and a simple readout circuit, but the drawbacks are a low repeatability and a sensitivity to temperature.[29] Touchpad sensors based on an infrared photosensing mechanism can detect the infrared light intensity changes caused by an approaching finger.[27] They show selective insensitivity to ambient light conditions, but the main issues are the complex fabrication process, high power consumption, and high cost. Compared to these mechanisms mentioned above, capacitive sensing has become popular mainly because of its low power consumption, the compact layout, simple device construction, high sensitivity, high repeatability, and immunity to temperature fluctuation.[1,14] Furthermore, current touchpad or tactile sensors, mainly based on polymer substrates with a smooth surface, like polydimethylsiloxane (PDMS) films, are less likely to be foldable. In sharp contrast, paper substrates provide more benefits for sensors, such as being ultrathin and foldable.[1,14,21] Other advantages of using paper substrates for sensors based on ion conductance change are the porosity and larger interfacial area, which could provide a higher sensitivity and faster response. Of course, the chemical stability of the paper substrate in the sensing environment and the compatibility to electrode materials should be carefully considered for an acceptable lifetime of device.[14]

Typically, a capacitive touch pad contains one or more capacitors in the touching area which register touch input by detecting relative variations in capacitance produced within the touching area. Touch pad capacitors can be of two types (parallel-plate capacitors and capacitors with electrodes in the same plate), depending on the structure of their active and grounded electrodes, but with both sharing a common sensing principle[13] (Figure 1a). Briefly, in the absence of human fingers (or other conductive objects) interacting with the sensor

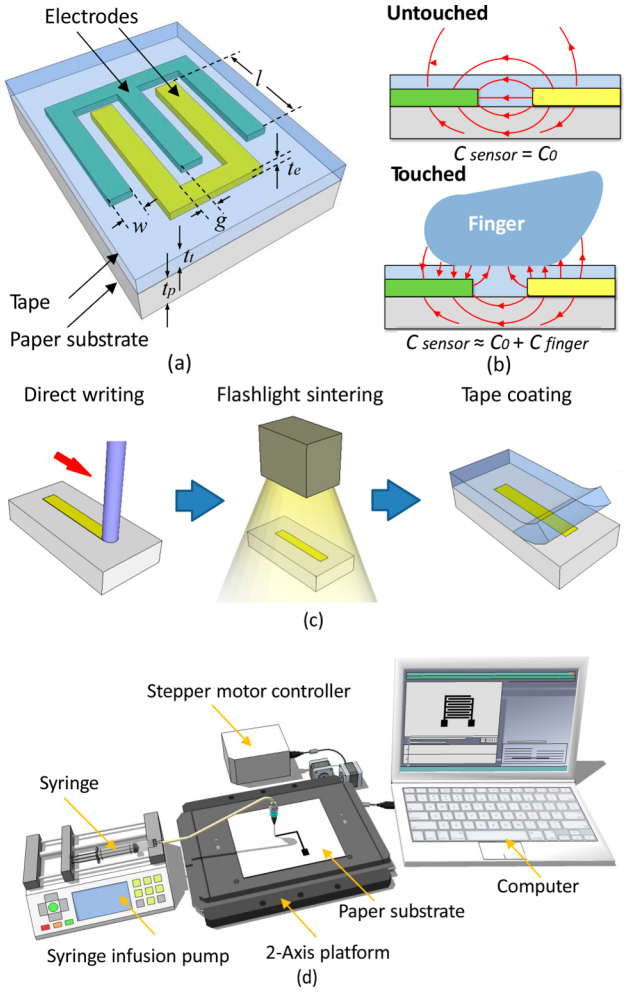

Figure 1. Paper-based touch pad. (a) Schematic view of a paper-based touch pad. (b) Working principle of the paper-based touchpad. (c) Fabrication of the paper-based touchpad involving direct writing silver nanowire ink, flashlight sintering and tape coating. (d) The schematic of the direct writing equipment.

surface, an intrinsic capacity value of C_0, mainly attributable to the electrode (Figure 1b) interactions between the capacitors electrical field and the surrounding medium. When a finger touches the sensor surface, it functionally grounds the electrodes, modifying the electrical field around the sensor to increase total capacitance roughly by the value associated with effective finger capacitance C_{finger}.

Previous studies demonstrate capacitors with electrodes in the same plate exhibit a relatively smaller initial capacitance than parallel-plate capacitors. Upon touch, capacitors with electrodes in the same plate increase capacitance by 1−2 orders, and thus are more sensitive than parallel-plate capacitors.[13] Capacitors with electrodes in the same plate enable 2D manufacturing on a single paper substrate, and are therefore the capacitors utilized throughout this work.

Figure 1a illustrates the geometrical design of interdigitated electrodes, comprising two comb-like electrodes, one grounded, the other active. A layer of polymer tape serves as the dielectric overlay and protects the capacitors. For a theoretical analysis of the capacitance in both untouched and touched states, we used finite element method (FEM) to compute electric field *E*, and "Gauss's law"[30] to calculate capacitance

$$C = \frac{Q}{\left|U_{\text{active}} - U_{\text{ground}}\right|} = \frac{\oiint_s \varepsilon\varepsilon_0 E dA}{\int_c E dl} \quad (1)$$

where Q is the total charge in each electrode, U_{active} and U_{ground} are (respectively) the electric potentials of two electrodes, and ε are the relative permittivity of the surrounding materials, the electric constant, s is the closed surface surrounding the electrodes, dA is an infinitesimal element of area, c is an arbitrary path connecting the two electrodes, and dl is an infinitesimal element in the path.

To monitor capacitance variation during touching, a signal generator is cascaded with a touchpad capacitor and a 100 kΩ resistor to form a "RC" circuit. The signal generator provides square waves to the RC, and an oscilloscope detects the potential change across the touchpad. Rise time, the time taken by a signal to change from a specified low to a specified high value, is proportional to the time constant of the RC circuit. By measuring rise time, capacitance can be calculated, as discussed in detail in the Results and Discussion section.

This proof-of-concept experiment is based on an Arduino system, a single-board microcontroller which makes building interactive objects more accessible. A single I/O pin discharge and internal pull-up strategy was conducted to achieve a simple and highly sensitive measurement (see Figure S3 in the Supporting Information). Relative to previous works,[13] this strategy provides relatively high sensitivity to a pF range while simplifying the detection circuit without the need for additional hardware.

3. EXPERIMENTAL SECTION

3.1. Preparation of Silver Nanowire ink. $AgNO_3$, NaCl, and ethylene glycol (EG) used for this study were purchased from Fisher Scientific International. Polyvinylpyrrolidone (PVP, average molecular weight (M_w) ≈ 40 000) powder was purchased from Sigma-Aldrich Corporation. All reagents were used without further purification.

Silver nanowires were synthesized in large scale via a polyol solution with PVP as a structure directing reagent.[23] In each synthesis, 10 mL of EG-based $AgNO_3$ solution (0.9 M) and 6 mL of EG-based NaCl solution (0.01 M) were added into 184 mL EG solution of PVP (0.284 M). Subsequently, the mixture was autoclaved at 195 °C for 15 min and then naturally cooled to room temperature.

The silver nanowire ink (5% silver nanowire by mass) was prepared via a washing and concentration process. The as-prepared silver nanowires were washed with deionized (DI) water to remove the ethylene glycol and PVP and twice condensed by centrifugation. Finally, the precipitate was collected and dispersed in ultrapure water (electrical resistivity approximately 18 MΩ/cm).

3.2. Direct Writing of Devices. Figure 1c summarizes the printing of the device, with the fabrication of paper capacitive touchpads using a direct writing system illustrated in Figure 1d. The paper substrates (Inkjet paper purchased from Scantron Corporation; photo and printing papers purchased from Office Depot, Inc.) were fixed on a program controlled 2-axis platform. The needle tip (0.35 mm external diameter) was in vertical contact with the upper paper surface. The opposite needle end was fed silver nanowire ink through a programmed syringe pump (Fusion 400, Chemyx Inc.). During writing, the syringe pump infused the ink onto the paper surface at a speed of 0.075 mL/min while the movement of the platform was controlled by Arduino. After writing, a camera flash light (TT660, NEEWER) sintering process was conducted with the light source fixed atop the sampler 1 cm from the paper surface. Several flash pulses illuminated the sample with an energy density of 4.6 J/cm^2 per pulse. Finally, single-side tape (3 M scotch tape, 3 M Company) was coated onto the surface of the sample, serving as an overlay.

4. RESULTS AND DISCUSSION

4.1. Characterizations of Silver Nanowire ink. The silver nanowires, which comprised ∼5% of the ink (w/w) were characterized by SEM (Figure 2a) as ∼15 μm long and 60 nm thick with an average aspect ratio of 300 (Figure 2c, d). Detailed silver nanowire morphology can be seen on a high-resolution image (Figure 2b), which reveals the cross-sectional pentagonal nanowire shape. These images suggest uniform nanowires can be obtained through the current synthetic approach.

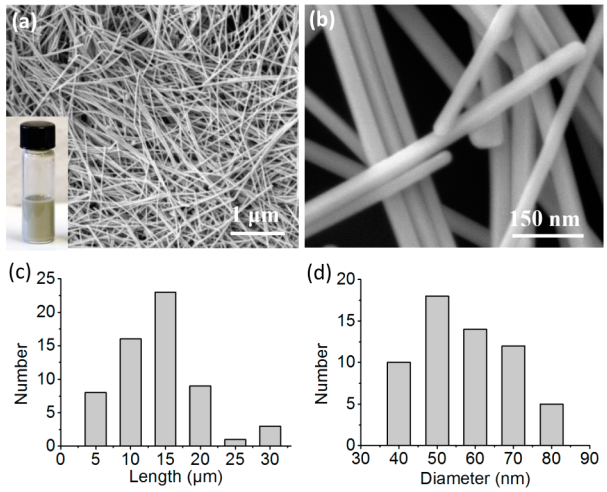

Figure 2. Silver nanowire ink. (a) SEM image of silver nanowire ink (inset is the silver nanowire ink in a vial.) (b) High-resolution SEM image of silver nanowire. (c) Length and (d) diameter distributions of the silver nanowire ink.

4.2. Photonic Sintering of Silver Nanowire Tracks. The as-prepared silver nanowire conductive track deposited on the printing paper substrate exhibits a relatively high resistance, in the few kΩ range, which slowly decreases to 1.95 kΩ after 24 h without any postprocessing. It has been widely recognized that silver nanowires with a high aspect ratio can exhibit good conductivity through the formation of conductive networks. Due to the high conductivity of silver, the sheet resistance of a silver nanowire network is largely a function of the resistance at internanowire junctions.[22,31] The postprocessing treatment in our work was conducted using a camera flash light source with an energy density of 4.6 J/cm^2 to lower the junction resistance between adjacent silver nanowires through sintering. Utilizing the plasmonic effect,[32] low light densities can be concentrated at gaps between two adjacent nano-objects to produce "hot-spots" without heating their surroundings, including the paper substrate.[22] This plasmonic heating effect, combined with the "melting point depression" phenomenon[18,33] associated with the nanoscale diameter of silver nanowires can successfully weld the nanowire networks at room temperature.

Sequential resistance changes during the flash sintering process provide further insight into sintering progression within silver nanowire networks on paper substrates (Figure 3a). The process employed a series of 5 flash pulses, sequentially denoted as pulses 1 through 5 interspersed with a 5s interval. The sheet resistance decreased continuously over the first three flash pulses, with the first pulse producing the most marked decrease in resistance from 2.15 kΩ to 830 Ω, followed by a further drop in resistance of 370 Ω after the second pulse. After

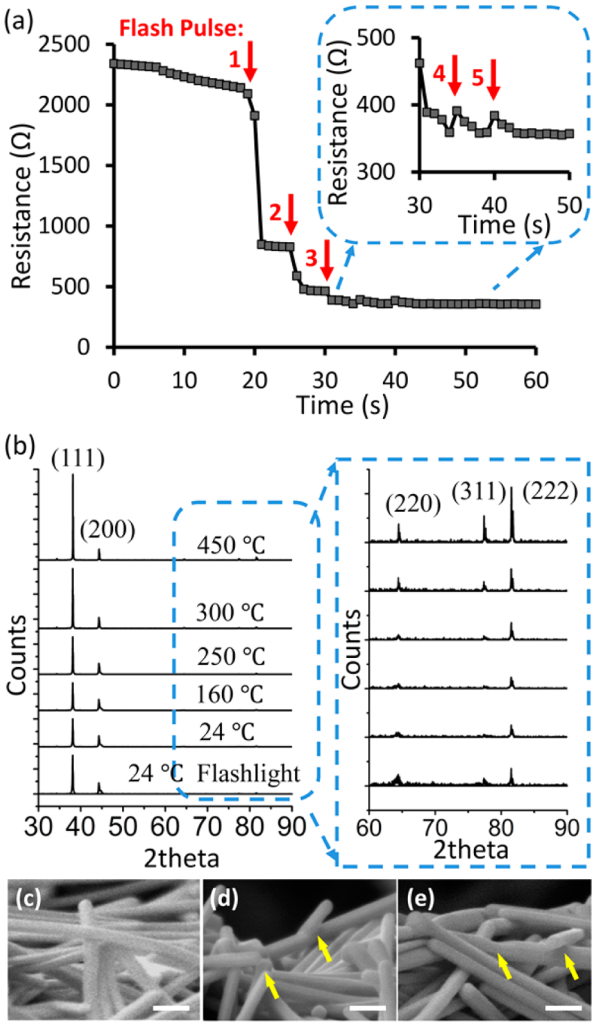

Figure 3. (a) Experimental results of in situ measured resistance of deposited silver nanowire conductive tracks during the flashlight sintering process, utilizing a flash light irradiation energy of 4.6 J/cm^2 per pulse. (b) XRD results of silver nanowire ink after postprocessing with either thermal sintering at a series of temperatures, or flashlight irradiation, spectrum is normalized to (200) peaks. SEM images of silver nanowire tracks on printing paper substrate (c) before sintering, after (d) photonic sintering and (e) thermal sintering at 250 °C for 5 min. The white scale bars indicate 150 nm.

the third pulse, the magnitude of the decrease in resistance declined, until finally stabilizing at 355 Ω, a resistance value 14.8% of that prior to photonic sintering.

Notably, fourth and fifth pulses only slightly influenced the final resistance of the conductive track, but it is worth mentioning that an instantaneous increase in resistance around 35 Ω was associated with the fourth and fifth pulse, which then changed to 355 Ω in 4 s. This can be attributed to the positive temperature coefficient for resistance of silver nanowire, and poor thermal conductivities of paper substrates and air. The plasmon resonance excited by flash pulses generates hot points with temperature change at silver nanowire junctions. This phenomenon is similar to one recently reported for copper nanoparticle films on a polyimide substrate.[34] The temperature and sheet resistance of copper nanoparticle films rapidly increase during flash illumination, and then decrease exponentially within several hundred of a millisecond, by about one order faster than was observed in the present study. These differences in temperature and sheet resistance between materials may be a function of silver nanowires tending to form reticular structures at lower densities, rather than a continuous higher-density film formed by individual nanoparticles.[34]

To determine the heating efficiency of the hot spot generated by photonic flash pulses, a comparative thermal (hot plate; sequentially up to 250 °C for 5 min) sintering experiment using silver nanowires on glass slides was evaluated using X-ray diffraction (D2 phaser, Bruker Corporation), the results of which are illustrated in Figure 3b. Sintering at silver nanowire junctions results in orientation changes leading to significantly increased peak heights of (111), (220), (311), and (222) commensurate with increasing temperatures. Flash sintering results in similar XRD patterns (i.e., the similar peak ratio relative to (200) peak) as that produced by thermal sintering at 250 °C for 5 min as confirmed by SEM images (Figure 3c–e). These results imply flash pulses generate a roughly 220 °C temperature increase above ambient temperatures at the nanowire junctions, which is nearly 120 °C higher than that for copper nanoparticles.[34] From an application perspective, this is important as it demonstrates silver nanowires in printed silver nanowire tracks, upon photonic sintering, close junctions between adjacent nanowires and improve conductance properties similar to sintering by heating to 250 °C for 5 min (Figure 3d). Notably, the color of printed silver nanowire ink transforms from dark gray to greyish yellow upon flash illumination, arising from morphological changes during the sintering process.[22]

4.3. Silver Nanowire Distribution on Paper Substrates. Surface topography of papers serving as substrates for printed silver nanowire ink modified their deposition and dispersion considerably (see Figure S1 in the Supporting Information). When photo paper was used as a substrate, silver nanowires adhered to the surface but formed a nanoporous film less than 1 μm in thickness because of the top waxy layer inherent to this type of paper (Figure 4). Conversely, inkjet and printing paper have much rougher surface properties with cellular surface fibers facilitating nanowire diffusion to about 5 μm, resulting in a relatively thick surface layer covered with silver nanowires (Figure 4b, c). Printed ink silver nanowires are probably limited in their diffusion range by their length (around 15 μm), with cellulose fibers serving as filters to limit silver nanowire diffusion beyond 5 μm, while also preventing their movement from the surface deeper into the paper matrix (see Figure S2a in the Supporting Information). A diffusion boundary of silver nanowires is shown by the dash line in Figure 4d, which incidentally also appeared to peel cellular fibers from the surface of the paper.

4.4. Electric Properties of Silver Nanowire Track. The amount of Ag-NWs per unit area of circuit can be characterized by areal density,[21] with a higher areal density of silver nanowires producing lower sheet resistance. Areal density can be varied by changing the injection rate, which can be optimized for each paper substrate to maximize conductivity (and minimize sheet resistance) relative to ink consumption (Figure 4e). Notably, silver nanowire tracks on photo paper substrates yielded the highest conductance properties, while those on printing paper show the lowest among the three paper types when evaluated with the same ink and identical writing speed. For each paper type, the sheet resistance initially decreases rapidly with increasing areal density, and then gradually plateaus with areal densities higher than 0.25 mg/

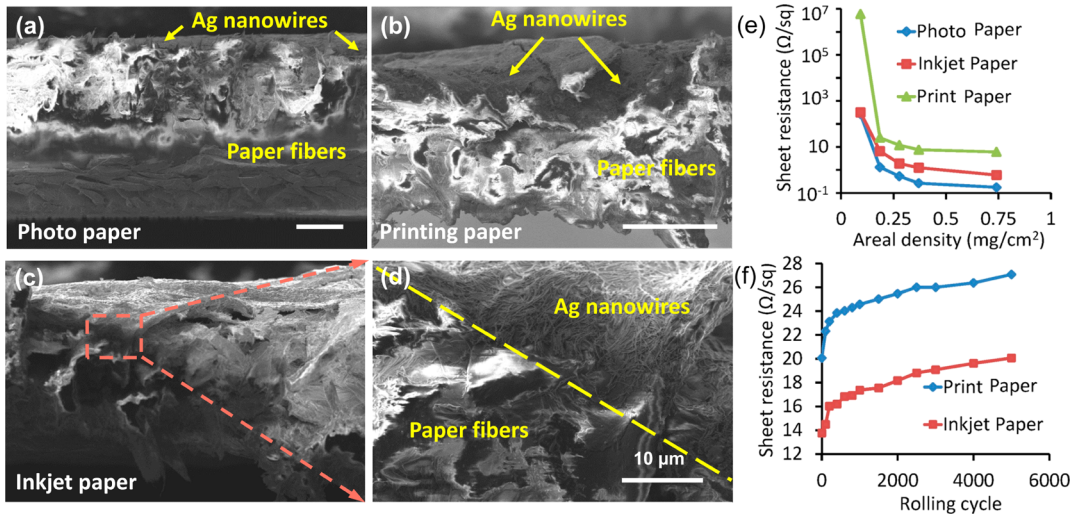

Figure 4. Cross-sectional SEM image of silver nanowire tracks on (a) photo paper, (b) printing paper, and (c) inkjet paper. The scale bars in a–c indicates 50 μm. (d) Higher-magnification image from c. Sheet resistance of silver nanowire conductive track as a function of (e) the areal density on three kinds of papers, and (f) rolling cycles with inkjet and printing papers.

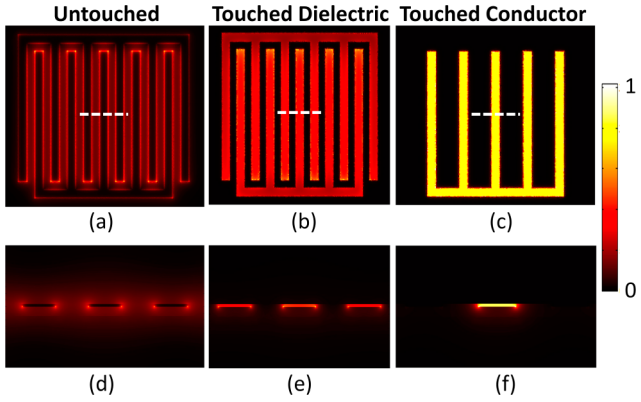

Figure 5. Top-down and cross-sectional views of normalized electric field distributions on the paper surface of a touchpad (a, d) without finger touching, (b, e) when touched by a "dry finger", and (c, f) when touched by a "wet finger". The white dash lines in a–c mark the positions of the cross-sectional views.

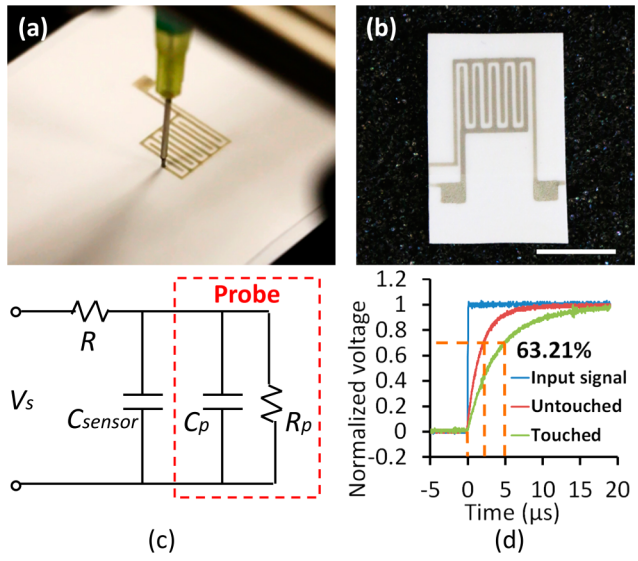

Figure 6. Images of (a) a touchpad during silver nanowire ink writing and (b) a completed touchpad on paper substrate. (c) Schematic circuit for the detection of touchpad capacitance with a signal generator and an oscilloscope (labeled only as probe in the image). (d) When applying a square wave across the RC circuit, the observed response with an increasing voltage between two ends of the touchpad. The orange dashed lines in d mark the time constant equivalent to the product of the resistance and capacitance of the circuit.

cm^2 for any of the three paper-based tracks. Consequently, an areal density of 0.278 mg/cm^2 was chosen as optimal for lowest sheet resistance, and factoring in ink conservation, for all three paper substrates.

Electrodes on flexible paper substrates must maintain their performance even when undergoing bending deformation, sometimes in applications demanding sharp bending radii. To investigate the bending stability of silver nanowire conductive tracks on paper substrates, rolling tests were conducted between two tracks written on both printing and inkjet paper. Printed samples were rolled back and forth by step motor across a rod of 6.5 mm radius with changes in resistance during the rolling process monitored. The electrode resistance on both paper substrates changed similarly during rolling (Figure 4f), with resistance increasing by nearly 50% in the first 500 cycles, with only modest increases in resistance thereafter. Notably, the conducting circuits did not fail after 5000 cycles, and no substantive differences can be seen between SEM images before and after rolling tests (see Figure S2 in the Supporting Information). Clearly, silver nanowire conductive tracks fabricated by direct writing are robust, with bending stabilities reliable under even exceptional applications.

4.5. Paper-Based Touchpad Electric Field Distributions. In our numerical calculations, the geometric parameters of a feasible paper-based touchpad built with electrodes was set with a width of 0.5 mm, tape thickness of 40 μm, and a paper thickness of 140 μm with an overlap length l ranging from 4 to 16 mm (Figure. 1a). We defined an "activated unit" as a U-shape grounded-electrode shell combined with an internal straight active electrode. The number of active units ranges from 2 to 10; the relative permittivity of paper and tape are assumed to be 4 and 3, respectively[1,35]

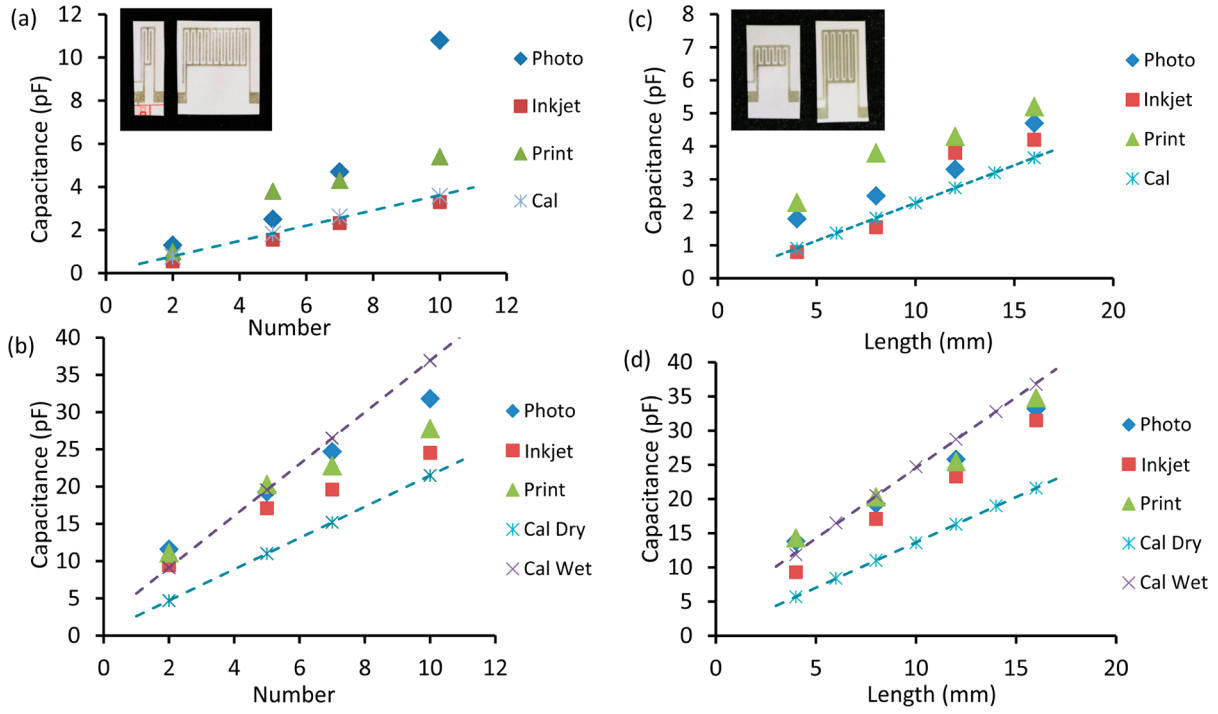

Figure 7. Influence of finger-electrode number on touchpad capacitances with various paper substrates in (a) untouched and (b) touched states; the influence of overlap length of active and grounded electrodes to touchpad capacitances of the various paper substrates in (c) untouched and (d) touched states. The inset images are photos of touchpads with different active electrode numbers and overlap electrode lengths. The dashed lines represent calculated results at two extreme finger conditions (lower, dry; and upper, wet).

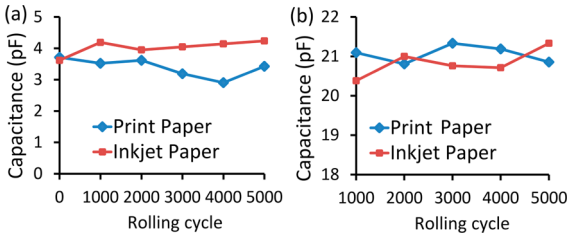

Figure 8. Touchpad capacitance on printing and inkjet paper during rolling cycles in (a) untouched and (b) touched states.

Figure 5a shows the paper surface electric field distributions on a touchpad in the absence of a finger touch. The electric field mainly concentrates in the gap between the active and grounded electrodes with an increased field density at the electrode edges as illustrated in the cross-sectional view, Figure 5d. Notably, there is almost no electric field on the top of electrodes and several "dark stripes" are thus formed. Both in-plane and cross-sectional views provide evidence of a relatively weak electric field existing in the absence of a finger touch.

However, when a finger is placed on a touchpad, despite there being no direct contact between the finger and the electrodes owing to the protective tape layer, the interaction between the finger and electrodes results in a capacitance, C_{finger}, between the finger and electrodes (Figure 1b). Simultaneously, the human body supporting the finger contributes electrical impedance, Z_b, with an approximate capacitance of 100 pF, and an approximate resistance of 1.5 kΩ to the ground.[13]

The theoretical modeling of a finger is complicated by variability in electrical properties of human fingers, which vary with personal conditions, and over time within an individual.[31] Herein, we greatly simplify the electrical properties of human fingers by applying two extreme cases, wet and dry fingers. If we consider the properties of a dry finger as a purely dielectric material, its relative permittivity is assumed to be 60,[36] which is less than the 80.2 permittivity of water.[37] Conversely, a wet finger is considered conductive with surface properties and permittivity commensurate with that of water.

Both top and cross-sectional views of the electrical field distributions of a touchpad upon touch with a dry finger on its surface demonstrate great electrical field enhancement in the tape layer between the finger and all electrodes (Figure 5b, e). It is notable that these electrodes are visible as "dark stripes" in the untouched condition. Conversely, when putting a wet finger on the touchpad, the electrical field largely concentrates within the gap between active electrodes, whereas the grounded electrodes remain dark (Figure 5c and 5f). In this scenario, the conductive finger, being grounded through the human body, possesses no potential difference, nor is there an electrical field generated between the finger and the grounded electrodes. However, the enhanced electrical potential difference between the active electrode and finger results in much higher electrical field intensity, more than two times larger than that generated by a dry finger interacting with a touchpad.

In practice, real human fingers would exhibit surface moistures intermediate between these two extremes, being neither completely nonconductive nor exhibiting perfect conductivity. We can safely conclude that when real fingers interact with touchpads, there is a higher electric field density generated between active electrodes and the interacting finger, and a lower electrical field density between grounded electrodes and the finger. The modeling of the finger interactions along with eq 1 provides a simplified means of predicting variation range in C_{finger} within a touch sensor design. Calculated

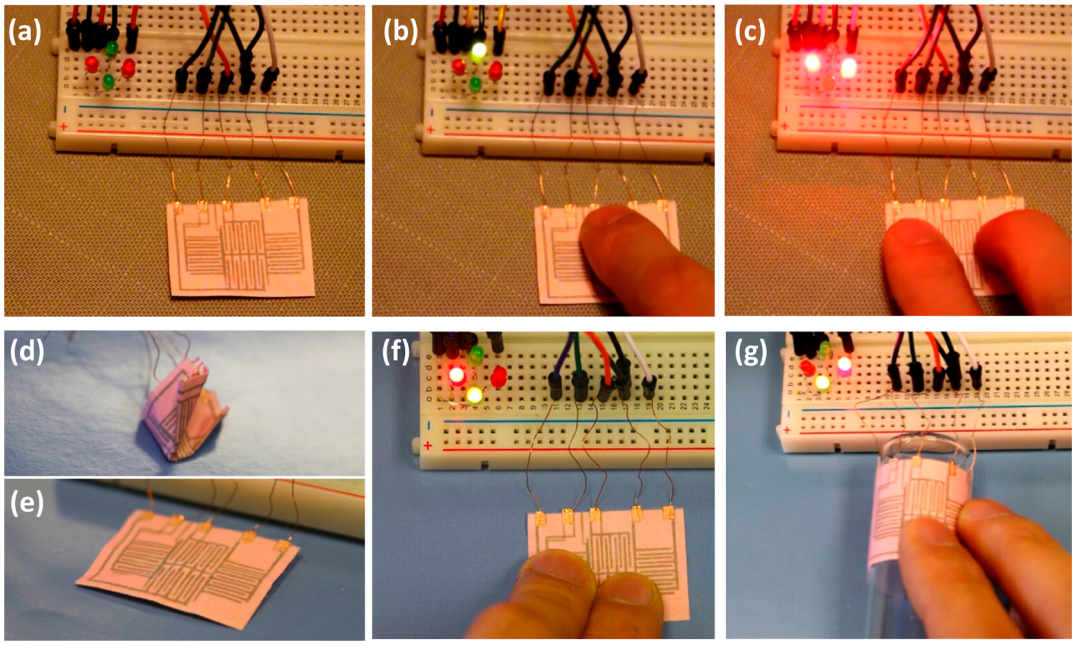

Figure 9. Four keypad touch pad in (a) untouched state, (b) touching with a single finger, (c) touching with two fingers. (d) Folded touch pad, (e) touch pad after 15 folding cycles, (f) unfolded touch pad with two fingers touching, (g) touch pad functioning on a curved surface.

capacitance and experimental results are in good agreement (Figure 7, 8) as discussed in the following sections.

4.6. Capacitance of Paper-Based Touchpads. During the writing process when a touchpad is being produced (Figure 6a), and once completed Figure 6b, the two thick side legs are clearly visible and serve as the connection to external circuits. Schematically (Figure 6c), a touchpad can be represented as a capacitor C cascaded with a 100 kΩ resistor R and a signal generator, with capacitance C_p and resistance R_p of the oscilloscope probe being 16 pF and 10 MΩ, respectively, which monitors the voltage across both touchpad electrodes. The output signal of a touchpad with an 8 mm overlap length and 5 activated units is shown in Figure 6d. The time constant is defined as that time for the voltage to rise to 1−1/e, or 63.21% of the high value.

The resistance of the whole system, Z, at frequency f satisfies the following equation

$$Z = R + \frac{1}{\frac{1}{R_p} + j\omega(C + C_p)} \tag{2}$$

where $\omega = 2\pi f$ is the angular frequency of the input signal.

The frequency f of a square wave comprises components of odd-integer harmonic frequencies (in the term of $2\pi(2k-1)f$). In our measurements, this value is much larger than 10 kHz, resulting in $1/R_p \ll \omega(C + C_p)$. Herein, we can negate $1/R_p$ and rewrite eq 3 as

$$Z = R + \frac{1}{j\omega(C + C_p)} = R + \frac{1}{j\omega C_{eq}} \tag{3}$$

where $C_{eq} = C + C_p$ is the equivalent capacitance of the entire circuit. The rise time t_τ measured by the oscilloscope is a factor 2.197 times that of the time constant τ.

$$t_\tau = 2.197\tau = 2.197RC_{eq} \tag{4}$$

Thus, the capacitance of the touchpad is calculated as

$$C = \frac{t_\tau}{2.197R} - C_p \tag{5}$$

From both eq 4 and Figure 6d, we can summarize that the finger touching results in a greater time constant.

We investigated the influences of the activated unit number on three types of paper substrates. Figure 7a and 7b demonstrate increasing capacitance as a function of activated unit number. Photo paper yields the highest capacitance while inkjet paper possesses the lowest capacitance. In the untouched state, capacitance is at a pF range, but when touched, capacitance increases by one order. As predicted by the theoretical analysis shown in the dashed lines in the figure, capacitance when in a touched state is intermediate between the "dry finger" and "wet finger" scenarios. As with the influence exerted by the number of activated units, increasing overlap length leads to a touch pad capacitance increase as shown in Figure 7c, d. Given that a button with a size of 1 cm^2 normally provides a better user experience, the structure of the touchpad with 5 activated units and 8 mm overlap length was selected in our research.

The stability of paper-based touchpads was evaluated by rolling trials using both printing and inkjet paper substrates. As shown in Figure 8a, after 5000 rolling cycles, the capacitance of the touchpads on inkjet paper showed only a slight increase, whereas capacitance was relatively stable on printing paper throughout the rolling trial; likely arising from structural differences associated with cellulose and hemicellulose composition and fiber length between these two kinds of papers. Notably, capacitance change between untouched (Figure 8a) and touched (Figure 8b) states was less than 10% of the initial value after 5000 rolling cycles, indicating excellent rolling stability for touchpads on both paper substrates.

4.7. Demonstration of a Prototype Device. As a demonstration of feasibility, a touchpad with four sensing areas (four keypads) connected with four LEDs on a breadboard and processed by an Arduino board was

constructed (Figure 9a). When one of the keypads is touched by a finger, the increase in keypad capacitance leads to an increase in rise time (see Figure S4 in the Supporting Information). Arduino reads this info and lights the relevant LED as shown in Figures 9b and SV2 (see the Supporting Information). Different keypads are able to respond simultaneously and trigger the corresponding LED (Figure 9b, c).

A touch pad was folded and unfolded for 15 cycles (Figure 9d, e), yet maintained its functionality (Figure 9f). Moreover, this touch pad can function properly on a curved surface with a 22.8 mm diameter, which corresponds to an angle of 150.8° (Figure 9g). This proof-of-concept experiment illustrates that this paper-based touch pad is suitable to serve as a capacitive sensor in medical point-of-care devices or an e-skin for a robotic control applications; it also may be used anywhere flexible, robust, and inexpensive touch control is desirable.[25,38−40]

5. CONCLUSIONS

In this article, we explored the feasibility of directly writing touchpads on variety of papers using silver nanowire ink and a 2D programmed printing machine with postdeposition sintering using a camera flash light. A theoretical model was proposed to elucidate the capacitive operating of touch pads, which closely approximated empirical data.

The successfully developed paper-based touchpads produced by direct writing with silver nanowire inks offer several distinct advantages over existing counterparts including: (1) low-cost and disposable, (2) rapid sintering (typically requiring 3 flash pulses and less than 20 s using a commercial camera flash), (3) ultrathin and ultralight (less than 0.1 mm thickness with printing and inkjet paper substrates and less than 60 mg for a single keypad on printing paper), and (4) flexible and robust, retaining electrical stability after 5000 rolling cycles, which is sufficient for a mobile devices and a myriad of additional applications.

■ ASSOCIATED CONTENT

Supporting Information

This section includes microscope and SEM image of silver nanowire tracks on paper, schematic of internal pull-up circuits, threshold for Arduino, and two videos about directing writing and demonstration of a touchpad. This material is available free of charge via the Internet at http://pubs.acs.org.

■ AUTHOR INFORMATION

Corresponding Author

*E-mail: ahu3@utk.edu. Tel: (865) 974-5993.

Notes

The authors declare no competing financial interest.

■ ACKNOWLEDGMENTS

We are grateful to discussion with Dr. Wenchao Zhou from the Department of Mechanical Engineering, University of Arkansas, and Dr. Chad Duty, from the Manufacturing Demonstration Facilities, Oak Ridge National Lab. We also thank Prof. J. A. M. Boulet and D. Bridges for the manuscript revision.

■ REFERENCES

(1) Tobjörk, D.; Österbacka, R. Paper Electronics. *Adv. Mater.* **2011**, *23*, 1935−1961.

(2) Glavan, A. C.; Martinez, R. V.; Subramaniam, A. B.; Yoon, H. J.; Nunes, R. M. D.; Lange, H.; Thuo, M. M.; Whitesides, G. M. Omniphobic "RF Paper" Produced by Silanization of Paper with Fluoroalkyltrichlorosilanes. *Adv. Funct. Mater.* **2014**, *24*, 60−70.

(3) Zhang, Y.; Lei, C.; Soo Kim, W. Design optimized membrane-based flexible paper accelerometer with silver nano ink. *Appl. Phys. Lett.* **2013**, *103*, 073304.

(4) Liu, X.; Mwangi, M.; Li, X.; O'Brien, M.; Whitesides, G. M. Paper-based piezoresistive MEMS sensors. *Lab Chip* **2011**, *11*, 2189−2196.

(5) Zschieschang, U.; Yamamoto, T.; Takimiya, K.; Kuwabara, H.; Ikeda, M.; Sekitani, T.; Someya, T.; Klauk, H. Organic Electronics on Banknotes. *Adv. Mater.* **2011**, *23*, 654−658.

(6) Dou, W.; Qiang Zhu, L.; Jiang, J.; Wan, Q. Flexible protonic/electronic coupled neuron transistors self-assembled on paper substrates for logic applications. *Appl. Phys. Lett.* **2013**, *102*, 093509.

(7) Kim, J. Y.; Park, S. H.; Jeong, T.; Bae, M. J.; Song, S.; Lee, J.; Han, I. T.; Jung, D.; Yu, S. G. Paper as a substrate for inorganic powder electroluminescence devices. *IEEE Trans. Electron Devices* **2010**, *57*, 1470−1474.

(8) Leonat, L.; White, M. S.; Głowacki, E. D.; Scharber, M. C.; Zillger, T.; Rühling, J.; Hübler, A.; Sariciftci, N. S. 4% Efficient Polymer Solar Cells on Paper Substrates. *J. Phys. Chem. C* **2014**, *118*, 16813−16817.

(9) Kaltenbrunner, M.; White, M. S.; Głowacki, E. D.; Sekitani, T.; Someya, T.; Sariciftci, N. S.; Bauer, S. Ultrathin and lightweight organic solar cells with high flexibility. *Nat. Commun.* **2012**, *3*, 770.

(10) Cheng, Q.; Song, Z.; Ma, T.; Smith, B. B.; Tang, R.; Yu, H.; Jiang, H.; Chan, C. K. Folding Paper-Based Lithium-Ion Batteries for Higher Areal Energy Densities. *Nano Lett.* **2013**, *13*, 4969−4974.

(11) Zhang, X.; Lin, Z.; Chen, B.; Sharma, S.; Wong, C.; Zhang, W.; Deng, Y. Solid-state, flexible, high strength paper-based supercapacitors. *J. Mater. Chem. A* **2013**, *1*, 5835−5839.

(12) Chang, H.; Liu, C.; Chen, W. Flexible Nonvolatile Transistor Memory Devices Based on One-Dimensional Electrospun P3HT:Au Hybrid Nanofibers. *Adv. Funct. Mater.* **2013**, *23*, 4960−4968.

(13) Mazzeo, A. D.; Kalb, W. B.; Chan, L.; Killian, M. G.; Bloch, J.; Mazzeo, B. A.; Whitesides, G. M. Paper-Based, Capacitive Touch Pads. *Adv. Mater.* **2012**, *24*, 2850−2856.

(14) Nery, E. W.; Kubota, L. T. Sensing approaches on paper-based devices: a review. *Anal. Bioanal. Chem.* **2013**, *405*, 7573−7595.

(15) Zhao, W.; Berg, A. Lab on paper. *Lab Chip* **2008**, *8*, 1988−1991.

(16) Hu, J.; Wang, S.; Wang, L.; Li, F.; Pingguan-Murphy, B.; Lu, T. J.; Xu, F. Advances in paper-based point-of-care diagnostics. *Biosens. Bioelectron.* **2014**, *54*, 585−597.

(17) Wang, Y.; Ge, L.; Wang, P.; Yan, M.; Ge, S.; Li, N.; Yu, J.; Huang, J. Photoelectrochemical lab-on-paper device equipped with a porous Au-paper electrode and fluidic delay-switch for sensitive detection of DNA hybridization. *Lab Chip* **2013**, *13*, 3945−3955.

(18) Yang, C.; Wong, C. P.; Yuen, M. M. F. Printed electrically conductive composites: conductive filler designs and surface engineering. *J. Mater. Chem. C* **2013**, *1*, 4052−4069.

(19) Shankar, R.; Groven, L.; Amert, A.; Whites, K. W.; Kellar, J. J. Non-aqueous synthesis of silver nanoparticles using tin acetate as a reducing agent for the conductive ink formulation in printed electronics. *J. Mater. Chem.* **2011**, *21*, 10871−10877.

(20) Zhu, Y.; Qin, Q.; Xu, F. R.; Fan, F.; Ding, Y.; Zhang, T.; Wiley, B. J.; Wang, Z. L. Size effects on elasticity, yielding, and fracture of silver nanowires: In situ experiments. *Phys. Rev. B* **2012**, *85*, 045443.

(21) Huang, G.; Xiao, H.; Fu, S. Paper-based silver-nanowire electronic circuits with outstanding electrical conductivity and extreme bending stability. *Nanoscale* **2014**, *6*, 8495−8502.

(22) Garnett, E. C.; Cai, W.; Cha, J.; Mahmood, F.; Connor, S. T.; Christoforo, M. G.; Cui, Y.; McGehee, M. D.; Brongersma, M. L. Self-limited Plasmonic Welding of Silver Nanowire Junctions. *Nat. Mater.* **2012**, *11*, 241−249.

(23) Peng, P.; Hu, A.; Huang, H.; Gerlich, A. P.; Zhao, B.; Zhou, Y. N. Room-temperature pressureless bonding with silver nanowire paste:

towards organic electronic and heat-sensitive functional devices packaging. *J. Mater. Chem.* **2012**, *22*, 12997−13001.
(24) Magdassi, S.; Grouchko, M.; Berezin, O.; Kamyshny, A. Triggering the Sintering of Silver Nanoparticles at Room Temperature. *ACS Nano* **2010**, *4*, 1943−1948.
(25) Segev-Bar, M.; Landman, A.; Nir-Shapira, M.; Shuster, G.; Haick, H. Tunable Touch Sensor and Combined Sensing Platform: Toward Nanoparticle-based Electronic Skin. *ACS Appl. Mater. Interfaces* **2013**, *5*, 5531−5541.
(26) Mannsfeld, S. C. B.; Tee, B. C. K.; Stoltenberg, R. M.; Chen, C. V. H. H.; Barman, S.; Muir, B. V. O.; Sokolov, A. N.; Reese, C.; Bao, Z. Highly Sensitive Flexible Pressure Sensors with Microstructured Rubber Dielectric Layers. *Nat. Mater.* **2010**, *9*, 859−864.
(27) Han, S. Y.; Jeon, K. S.; Cho, B.; Seo, M. S.; Song, J.; Kong, H. S. Characteristics of a-SiGe: H thin film transistor infrared photosensor for touch sensing displays. *IEEE J. Quantum Electron.* **2012**, *48*, 952−959.
(28) Yang, Y.; Zhang, H.; Zhong, X.; Yi, F.; Yu, R.; Zhang, Y.; Wang, Z. L. Electret Film-Enhanced Triboelectric Nanogenerator Matrix for Self-Powered Instantaneous Tactile Imaging. *ACS Appl. Mater. Interfaces* **2014**, *6*, 3680−3688.
(29) Tiwana, M. I.; Redmond, S. J.; Lovell, N. H. A review of tactile sensing technologies with applications in biomedical engineering. *Sens. Actuators, A* **2012**, *179*, 17−31.
(30) Jackson, J. D. *Classical Electrodynamics*, 3rd ed.; John Wiley: New York, 1999.
(31) Mutiso, R. M.; Sherrott, M. C.; Rathmell, A. R.; Wiley, B. J.; Winey, K. I. Integrating Simulations and Experiments To Predict Sheet Resistance and Optical Transmittance in Nanowire Films for Transparent Conductors. *ACS Nano* **2013**, *7*, 7654−7663.
(32) Zhang, X.; Hu, A.; Zhang, T.; Lei, W.; Xue, X.; Zhou, Y.; Duley, W. W. Self-Assembly of Large-Scale and Ultrathin Silver Nanoplate Films with Tunable Plasmon Resonance Properties. *ACS Nano* **2011**, *5*, 9082−9092.
(33) Hu, A.; Guo, J. Y.; Alarifi, H.; Patane, G.; Zhou, Y.; Compagnini, G.; Xu, C. X. Low temperature sintering of Ag nanoparticles for flexible electronics packaging. *Appl. Phys. Lett.* **2010**, *97*, 153117.
(34) Park, S. H.; Chung, W. H.; Kim, H. S. Temperature changes of copper nanoparticle ink during flash light sintering. *J. Mater. Process. Technol.* **2014**, *214*, 2730−2738.
(35) McKay, T. G.; Calius, E.; Anderson, I. A. The Dielectric Constant of 3M VHB: a Parameter in Dispute. In *Electroactive Polymer Actuators and Devices (EAPAD)*; SPIE: Bellingham, WA, 2009.
(36) Gabriel, S.; Lau, R. W.; Gabriel, C. The dielectric properties of biological tissues: III. Parametric models for the dielectric spectrum of tissues. *Phys. Med. Biol.* **1996**, *41*, 2271−2293.
(37) Murran, M. A.; Najjaran, H. Capacitance-based droplet position estimator for digital microfluidic devices. *Lab Chip* **2012**, *12*, 2053−2059.
(38) Chatterjee, D.; Shepherd, H.; Garrell, R. L. Electromechanical model for actuating liquids in a two-plate droplet microfluidic device. *Lab Chip* **2009**, *9*, 1219−1229.
(39) Peng, C.; Zhang, Z.; Kim, C. J.; Ju, Y. S. EWOD (electrowetting on dielectric) digital microfluidics powered by finger actuation. *Lab Chip* **2014**, *14*, 1117−1122.
(40) Lipomi, D. J.; Vosgueritchian, M.; Tee, B. C.; Hellstrom, S. L.; Lee, J. A.; Fox, C. H.; Bao, Z. Skin-like pressure and strain sensors based on transparent elastic films of carbon nanotubes. *Nat. Nanotechnol.* **2011**, *6*, 788.